Substrate Effects on Two-Dimensional Laser Beam Backscattering

H. F. Nelson* and D. C. Look Jr.†
University of Missouri—Rolla, Rolla, Missouri

Experimental measurements of backscattering from media with optical depths ranging from thin to thick and composed of anisotropic scattering particles exposed to a laser beam are presented. The laser beam is incident normal to the first surface of a scattering medium whose substrate is a diffuse reflector. Measurements are made for two substrates (white – nearly 100% reflecting, and black – nearly 100% absorbing) to study the effect of substrate reflection on backscatter. Latex particles of uniform size (diameter = 0.18 μm) are used as scattering centers in a water solution to create the scattering medium. Results are presented for backscattered radiation in the normal direction as a function of optical radius from the laser beam, optical thickness of the scattering medium, and the character of the substrate for albedos near one. It is shown that the character of the substrate can be important for optical depths up to 20. The white reflecting substrate always produces greater backscattered radiation than the black absorbing substrate when effects of the substrate are detectable. A correlation is developed that predicts the onset of substrate effects on the backscattered radiation as a function of optical radius and optical depth.

Nomenclature

c = effective scattering coefficient, $6C_{sca}/(\pi d^3)$
C_{sca} = scattering cross section
d = scattering particle diameter
g = asymmetry parameter
$G_{\exp}$ = experimental universal function, $r^2 I_{\exp}/(r_0^2 I_i)$
I_N = theoretical intensity leaving the medium normal to the surface at $z = 0$
I_i = magnitude of the incident intensity at $z = 0$
$I_{\exp}$ = measured intensity leaving the medium normal to the surface at $z = 0$
L = scattering medium depth
n = refractive index of the liquid carrier medium (1.33)
N = scattering particle number density
$P(\Theta)$ = scattering phase function
P_i = input power on the medium at $z = 0$ surface
r = radial distance from the center of laser beam
r_o = effective radius of laser beam
R = scattering medium radius
R_0 = aperture radius of detector probe
V = detector voltage
x = particle size parameter, $(n\pi d/\lambda_0)$
z = distance into the scattering medium (normal to upper surface)
$\delta(t)$ = Dirac delta function
η = particle volume concentration
θ = polar angle of incident intensity
$\bar{\theta}$ = effective acceptance angle of detector
Θ = angle between incident and scattered directions
κ = absorption coefficient of scattering medium
μ = $\cos\theta$
λ_0 = wavelength of laser beam in air, 0.6328 μm
ρ_N = normal reflectance, $(n-1)^2/(n+1)^2$
τ_r = radial optical thickness
τ_0 = optical depth of scattering medium to the substrate
τ_{r_0} = optical radius of incident laser beam
τ_R = optical radius of the scattering medium
ϕ = azimuth angle of incident laser beam
ω = single scattering albedo

Superscript
* = effective quantity that takes into account the effect of anisotropic scattering and albedo

Received April 8, 1987; presented as Paper 87-1483 at the AIAA 22nd Thermophysics Conference, Honolulu, HI, June 8-10, 1987; revision received Sept. 2, 1987.

*Professor of Aerospace Engineering, Thermal Radiative Transfer Group, Department of Mechanical and Aerospace Engineering. Associate Fellow AIAA.

†Professor of Mechanical Engineering, Thermal Radiative Transfer Group, Department of Mechanical and Aerospace Engineering. Associate Fellow AIAA.

MULTIDIMENSIONAL multiple scattering is significant when radiation is transferred in dust clouds and rocket plumes. Thermal radiation reflection and transmission in dust clouds from near-surface nuclear bursts are important not only for military damage assessment but also for understanding the resulting climatic effects. A facet of stealth technology is based on understanding the effect of particulate scattering of radiation on infrared rocket plume signatures. These applications of multiple scattering involve not only directional effects but also intensity magnitudes.

A simple situation used to investigate two-dimensional multiple scattering is the backscattering of a laser beam from a medium when the laser beam is incident normal to the surface of the medium. Numerical results are available for both semi-infinite[1-3] and finite thick media.[4,5] The scattering phase function in all of these studies is composed of a spike in the forward direction superimposed on an isotropic,[1-4] linear,[2-5] or Rayleigh[3] phase function. These results are obtained for the assumption that the refractive index of the scattering medium is one.

There are a limited number of multidimensional, multiple scattering experimental studies in which well-defined scattering particles were used.[6-10] Look et al.[6] reported good agreement between theory and experiment for the backscattering of a laser beam from a simulated semi-infinite medium. The medium was composed of distilled water and uniformly sized latex particles, $(0.035 \le d \le 1.011$ μm). The albedo was assumed to be one. A correlation factor $(1-g)$ was used to produce agreement between the anisotropic scattering experimental results and isotropic scattering theory. The backscattered intensity was presented as a function of the radial optical distance from the beam. Preliminary investigations of the backscattered radiation of a laser beam from a finite-depth medium were published in Refs. 7 and 8. In these investigations, 0.261 μm diam latex particles were used as the scattering centers. In Ref. 7, the particles were suspended in either distilled water or ethylene glycol to determine the influence of the refractive index of the liquid carrier. In Ref. 8, two laser

wavelengths were used: 0.4414 and 0.6328 μm. The results indicated an influence of the liquid carrier refractive index. At 0.6328 μm, an increase in the refractive index of the liquid reduced the backscattered radiation, whereas at 0.4414 μm, an increase in the liquid refractive index produced an increase in the backscattered radiation. The purpose of Ref. 10 was to extend the results of Refs. 7 and 8. In addition, Ref. 10 reported the sensitivity of the backscattered radiation to small changes in the albedo when the albedo is near 1 and considered the effects of the refractive index discontinuity at the boundary.

Theoretical Analysis

This paper presents experimental measurements of the backscattering from scattering media ranging from optically thin to optically thick with either a reflecting or an absorbing substrate. However, it is necessary to present a short review of the theoretical background for this research,[1-5] since the theoretical analysis presents considerable insight into the data reduction and presentation of the experimental results. The theoretical solution is available only for the absorbing substrate situation; consequently, it will be used to compare with the absorbing substrate experimental results to verify the experimental methods. The reflecting substrate results will not agree with the theory when the backscatter is sensitive to the substrate.

Figure 1 is a schematic of the physical situation that is being investigated. The laser beam is incident on a scattering medium with finite depth in which it undergoes multiple scattering. The theoretical development is based on the following assumptions: steady state, coherent scattering, negligible interference and polarization effects, homogeneous medium, no emission, refractive index of one, and two-dimensional cylindrical geometry.

Incident Radiation

For this investigation, the laser beam intensity was assumed to be Gaussian[11] so that it was given by

$$I^+(\tau_r, \mu, \phi) = I_i \delta(\mu - 1)\delta(\phi) \exp(-\tau_r^2/\tau_{r_0}^2) \qquad (1)$$

in which

$$\tau_r = (NC_{sca} + \kappa)r \quad \text{and} \quad \tau_{r_0} = (NC_{sca} + \kappa)r_o \qquad (2)$$

The Dirac delta-function product restricts the incident radiation to the normal direction. The resulting incident radiative flux is $I_i \exp(-r^2/r_0^2)$.

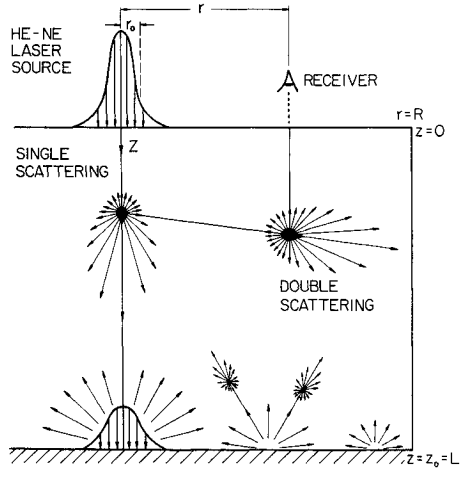

Fig. 1 Schematic of the two-dimensional, finite-depth scattering situation.

Scattering Phase Function

The particle size parameter x is the dimensionless ratio of the scattering particle circumference to the wavelength of the incident radiation. It can be used to characterize the scattering. Mie theory gives the exact solution for scattering by an arbitrary sphere. In the limit as x goes to zero, Mie theory yields the Rayleigh theory solution as the limiting approximation. For x less than about 0.3, Rayleigh theory is a reasonably good approximation. For x greater than about 0.3, Mie theory must be used for the scattering phase function. Mie theory phase functions typically have a strong forward-scattering lobe. The lobe becomes more intense as x increases.

The present investigation presents data from 0.18 μm diam latex particles suspended in distilled water, subjected to HeNe laser radiation ($\lambda_0 = 0.6328$ μm), so that $x = 1.19$. Figure 2 shows the Mie theory scattering phase function as a function of scattering angle. Note the development of a rather broad forward-scattering lobe. Measurements of the scattering phase functions of latex particles have been shown to be in excellent agreement with Mie theory.[12] Theoretically, this type of phase function can be approximated by

$$P(\Theta) = (1 - g) + 2g\,\delta(1 - \cos\theta) \qquad (3)$$

in which g is the asymmetry parameter.[13]

$$g = 0.5 \int_0^\pi \cos\Theta\, P(\Theta) \sin\Theta\, d\Theta \qquad (4)$$

When g is zero, the scattering is isotropic. When g approaches one the scattering becomes strong-forward.

The approximate phase function given by Eq. (3) is also shown in Fig. 2. The value of g is 0.25 for the 0.18 μm particles. The delta function, isotropic phase function of Eq. (3) approximates the backscattering quite well; however, it shows considerable error in the forward scattering. The phase function approximation given by Eq. (3) typically models the exact phase function more accurately for larger g values. Equation (3) is used in this research to model the scattering phase function because it has been used successfully in the two-dimensional, multiple scattering theory of Crosbie and Dougherty.[1-5] More complicated models similar to that of Eq. (3) are available for the phase function,[14] but they have not yet been incorporated into the two-dimensional, multiple scattering theoretical solutions.

Solution of Transport Equation

Using the phase function given by Eq. (3) in the equation of transfer yields a modified transfer equation similar to that for

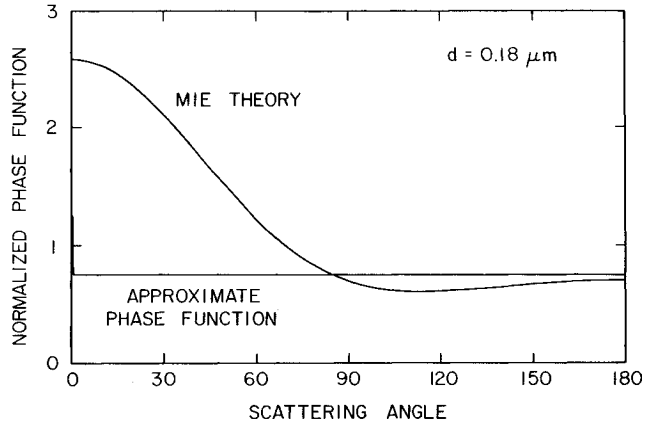

Fig. 2 Normalized phase function vs scattering angle for 0.18 μm latex particles at $\lambda_0 = 0.6328$ μm in water—Mie theory and delta-function isotropic approximation.

isotropic scattering in terms of the following modified optical coordinates and parameters:[1]

$$\tau_r^* = (1 - \omega\, g)\tau_r, \qquad \tau^*_{r_0} = (1 - \omega g)\tau_{r_0}$$

$$\tau_0^* = (1 - \omega\, g)\tau_0, \qquad \omega^* = \omega(1 - g)/(1 - \omega g)$$

$$\tau_R^* = \tau_0^*/(L/R) \tag{5}$$

in which

$$\tau_0 = (NC_{sca} + \kappa)L \quad \text{and} \quad \omega = NC_{sca}/(NC_{sca} + \kappa)$$

Thus, for anisotropic scattering with a phase function like Eq. (3), the isotropic solutions for the source function, flux, and intensity can be used by adjusting (scaling) the optical coordinates and the albedo according to Eqs. (5).[1,14]

This approximation has been used in one-dimensional, multiple scattering[15-18] and is generally accepted in the treatment of anisotropic scattering. Van de Hulst[13] noted that the scaling procedure is easy to use and, therefore, it is appealing for industrial design applications.

The exact two-dimensional integral equation describing the source function for the modified transfer equation was solved using separtation of variables and superposition. The solution for the backscattered intensity normal to the surface when r/r_0 is greater than about 5 is[1,3]

$$I_N(\tau_r^*) = I_i(r_0/r)^2\, G(\tau_r^*;\omega^*,\tau_0^*) \tag{6}$$

where

$$G(\tau_r^*;\, \tau_0^*) = \frac{\omega^*}{8\pi}\int_0^\infty tJ_0(t)R\left(\frac{t}{\tau_r^*};\, \omega^*,\, \tau_0^*\right) dt \tag{7}$$

The quantity $\omega^* J_0(t)R(t/\tau_r^*;\omega^*,\tau_0^*)/4$ is the intensity leaving normal to the medium when the medium is exposed to radially varying collimated radiation. Equations (6) and (7) have been evaluated numerically for a wide range of parameters in Refs. 1 and 3.

The theory was developed assuming a refractive index of one, which may be questionable; however, the assumption has been used previously since it significantly reduces the numerical complexity.[6,10] A single and double scattering analysis, including the effect of the refractive index, shows that the backscattered intensity should be reduced by $(1 - \rho_N)^2/n^2$. Therefore, τ_r^* is shifted by $(1 - \rho_N)^2/n^2$. This approximation is strictly valid only in the thin optical radii region, because a reduction in the reflected intensity at small optical radii dictates an increase in the intensity at large optical radii. The trends of this interface model are correct, even though it is a very simple model. It has been shown to improve the agreement between experiment and theory.[10]

Experimental Procedure

The experiment was designed to model a cylindrically symmetric, finite-depth scattering medium as indicated schematically in Fig. 1. Two glass tanks (17.0 and 26.6 cm in diameter) were used to contain the scattering medium. The tanks were fitted with two interchangeable bottoms; one was sprayed with a highly absorbing, diffusely reflecting black paint with a reflectance of less than 2%. The other was sprayed with a diffuse, highly reflecting white paint with a reflectance of more than 98%. The bottoms could be raised or lowered in the glass tank so that the depth of the scattering medium was adjustable.

The scattering medium was composed of 0.18 μm diam spherical latex particles immersed in distilled water. The amount of scattering was controlled by the concentration of latex particles. The laser beam ($\lambda_0 = 0.6328$ μm) was incident normal to the upper surface of the scattering medium.

Data Reduction

The data analysis follows quite closely Refs. 6 and 10; however, the magnitudes of some of the experimental parameters are different. The ratio of the reflected intensity to the incident laser beam intensity is

$$\frac{I_{exp}}{I_i} = \frac{1.53(10^{-7})}{\pi}\left(\frac{r_0}{\bar{\theta} R_0}\right)^2 \frac{V}{P_i} \tag{8}$$

in which $\bar{\theta} = 2.10$ deg, $R_0 = 0.169$ cm, $r_0 = 0.20$ cm, V is in volts, and P_i is in watts. This equation is very sensitive to the magnitudes of $\bar{\theta}$, R_0, and r_0. The r_0 sensitivity was eliminated by rearranging Eq. (8)

$$\frac{r^2 I_{exp}}{r_0^2 I_i} = G_{exp} = 0.001273\, r^2\, V/P_i \tag{9}$$

where G_{exp} is the experimental equivalent of the theoretical function G in Eq. (7).

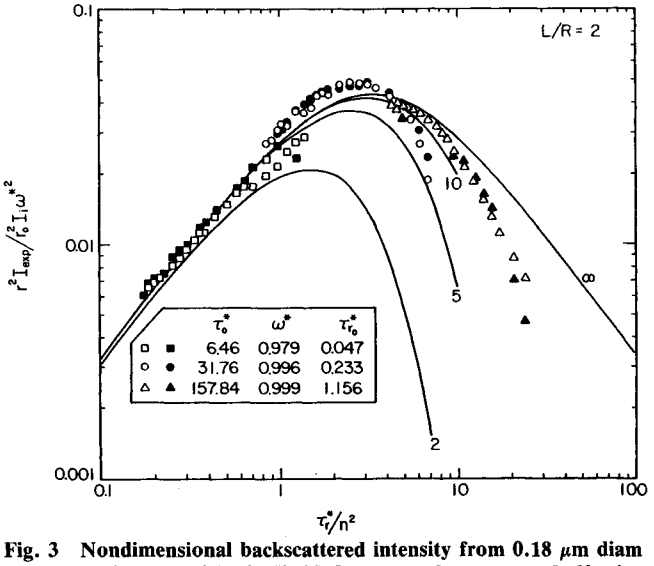

Fig. 3 Nondimensional backscattered intensity from 0.18 μm diam polystyrene latex particles in distilled water vs the contracted effective optical radius (L = 26.6 cm; R = 13.3 cm; solid symbols, white substrate; open symbols, black substrate).

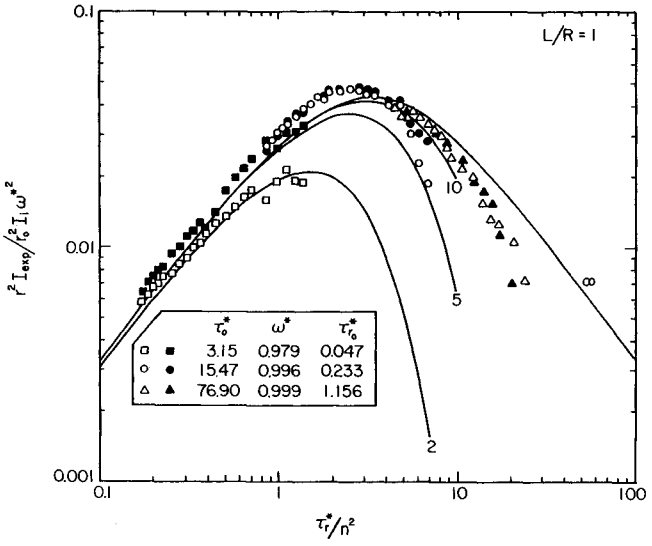

Fig. 4 Non dimensional backscattered intensity from 0.18 μm diam polystyrene latex particles in distilled water vs the contracted effective optical radius (L = 13.3 cm; R = 13.3 cm; solid symbols, white substrate; open symbols, black substrate).

It is convenient to write the optical thickness in terms of the particle volume concentration

$$\eta = N\pi d^3/6 \tag{10}$$

The optical radius and albedo become

$$\tau_r = \left(\eta\frac{6C_{sca}}{\pi d^3} + \kappa\right)r = (\eta c + \kappa)r \tag{11}$$

and

$$\omega = \eta c/(\eta c + \kappa) \tag{12}$$

The value of κ for distilled water was taken to be 0.005 1/cm at 0.6328 μm.[19] This number is somewhat questionable because of difficulties in measuring κ when κ is small, as well as difficulties in controlling water purity.

To compare the black substrate experimental data to theory, the actual experimental optical radius for the anisotropic case τ_r was multiplied by $(1-\omega g)$ and divided by the square of the medium index of refraction to yield the corresponding contracted effective optical radius for the theoretical isotropic case, τ_r^*/n^2. The $(1-\omega g)$ factor approximately transforms anisotropic scattering to an effective isotropic scattering situation, whereas the $1/n^2$ adequately accounts for effects of the index of refraction at the boundary. The value of n was assumed to be 1.33.

Particle Characterization

The latex particles that were used as scattering centers had a listed mean diameter of 0.18 μm; however, their size distribution was not uniform. The particles had a density of approximately 1.05 g/cm^3, but no settling was observed during the experiment. Their refractive index was 1.593. They were assumed to have a single scattering albedo of one. The characterization of these particles is given in Ref. 10. Experimental values were used for c, whereas the theoretical values of x and g were used. The x and g values were obtained by assuming a uniform size distribution at the manufacturer's stated size of 0.18 μm ($x = 1.19$, $g = 0.25$, and $c = 4850$ 1/cm).[10]

Results and Discussion

The intent of this study is to investigate the backscattering in the normal direction from finite optically thick media with black or white diffusely reflecting substrates in the presence of strong scattering. Figures 3–11 present G_{exp}/ω^{*2} vs τ_r^*/n^2 for τ_0^* values ranging from 0.28 to 158 for both white and black

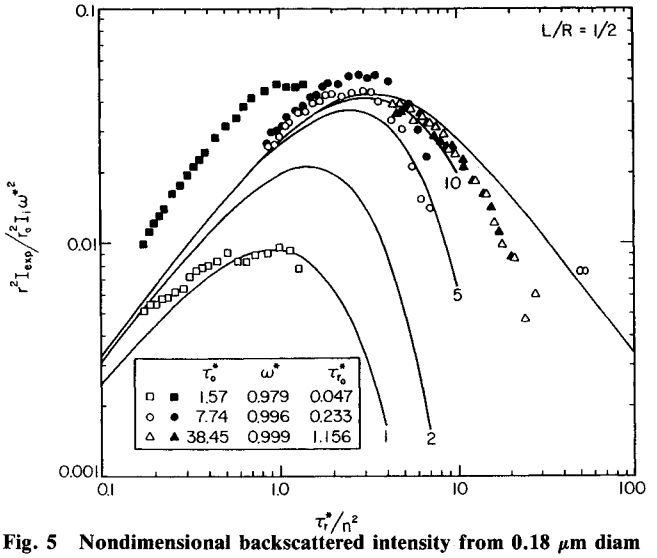

Fig. 5 Nondimensional backscattered intensity from 0.18 μm diam polystyrene latex particles in distilled water vs the contracted effective optical radius. ($L = 6.65$ cm; $R = 13.3$ cm; solid symbols, white substrate; open symbols, black substrate).

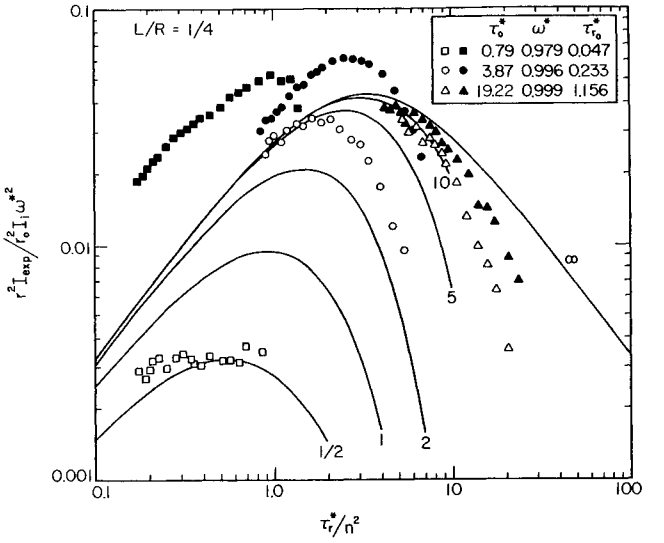

Fig. 6 Nondimensional backscattered intensity from 0.18 μm diam polystyrene latex particles in distilled water vs the contracted effective optical radius. ($L = 3.325$ cm; $R = 13.3$ cm; solid symbols, white substrate; open symbols, black substrate).

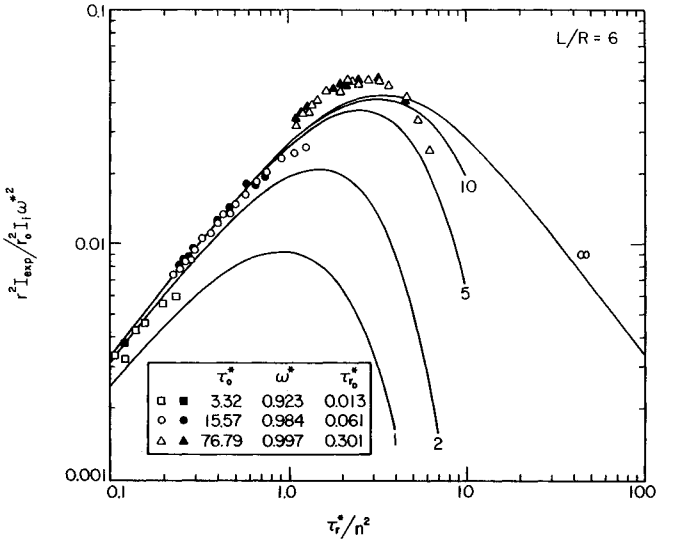

Fig. 7 Nondimensional backscattered intensity from 0.18 μm diam polystyrene latex particles in distilled water vs the contracted effective optical radius. ($L = 51$ cm; $R = 8.5$ cm; solid symbols, white substrate; open symbols, black substrate).

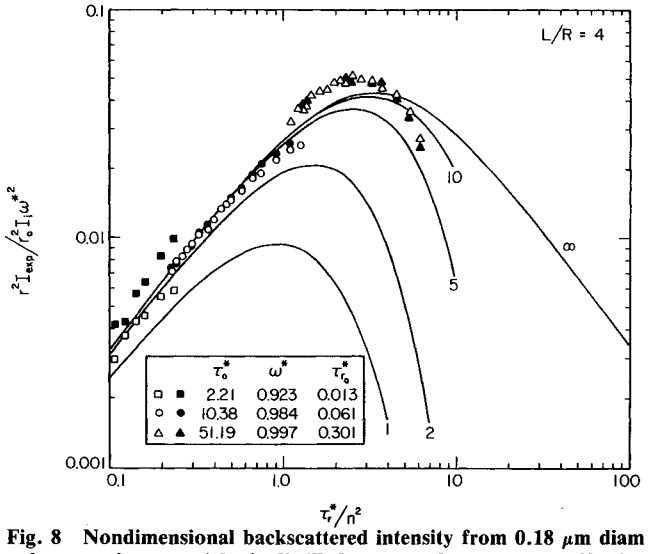

Fig. 8 Nondimensional backscattered intensity from 0.18 μm diam polystyrene latex particles in distilled water vs the contracted effective optical radius. ($L = 34$ cm; $R = 8.5$ cm; solid symbols, white substrate; open symbols, black substrate).

substrates. The effective albedo is greater than 0.923 for all the cases shown. The black substrate data are included for experimental verification. Each figure contains three sets of data for the white substrate and three sets of data for the black substrate. The values of ω^* and τ_R^* for each of the three data sets are the same for each figure, whereas τ_0^* is different for each set. The same scattering medium was used for each specific set of ω^* and τ_R^* values, and the depth was changed by raising the bottom to change the value of τ_0^*. Data are presented over the radial range from approximately $4\tau_{r0}^* < \tau_r^* < 20\tau_{r0}^*$. The solid lines on the figures represent the black substrate theoretical results for values of τ_0^* of ∞, 10, 5, 2, 1, and ½.

Substrate Effects

Figures 3–6 show the black and white substrate data for the scattering media with the largest radius. The values of τ_R^* are 3.15, 15.47, and 76.90 as one moves from the optically thinnest to the thickest scattering medium, respectively. Figure 3 gives the results for a scattering media with L/R equal to 2. The characteristics of the bottom do not influence the backscattered radiation detected at the upper surface in the normal direction, even for τ_0^* values as low as 6.5.

Figure 4 exhibits the data for a scattering medium when L/R equals 1. In this case, the backscattered radiation for τ_0^* greater than 15.5 is the same for both the black and white substrate. However, for τ_0^* equal to 3.2, the backscattering when the medium has white substrate is somewhat higher than that for the black substrate.

Figure 5 illustrates the backscattered radiation when L/R equals ½. The results are independent of the substrate when τ_0^* equals 38.5; however, the backscatter for τ_0^* equals 7.7 and 1.6 are highly dependent on the substrate characteristics. The white substrate yields considerably more backscattering near the incident laser beam than the black substrate does for these τ_0^* values.

Figure 6 presents data for a scattering medium with an L/R equal to ¼. The substrate characteristics are very important for this scattering medium. Substrate characteristics even affect the backscattering for τ_0^* equal to 19.2 (a rather large optical depth).

Figures 7–11 show data similar to that of Figs. 3–6, but they were taken in a smaller-diameter tank. The values of τ_R^* were 3.15, 15.47, and 76.9 as one moves from the optically thin to the optically thick medium, respectively. The data show the same trends that were previously discussed. Figure 7, for L/R equal to 6, does not show effects of the different substrates, even for τ_0^* as small as 3.32. The influence of the substrate begins to show up in Fig. 8 ($L/R = 4$) for $\tau_0^* = 2.21$. Figure 9 gives data for L/R equal to 2. The effect of substrate reflectance shows up only for $\tau_0^* = 1.11$. At $\tau_0^* = 5.2$, there are no detectable substrate effects. Figure 10, for L/R equal to 1, shows that the different substrates effect the normally backscattered radiation for τ_0^* up to a value of 2.60. The effects of changing the substrate show up for all the data shown in Fig. 11 for $L/R = ½$.

The preceding data on substrate effects can be summarized by plotting the value of τ_r^* where substrate effects become noticeable as a function of τ_0^*/ω^*, as shown in Fig. 12. Figure 12 shows τ_r^*/n^2 as a function of $(\tau_0^*/\omega^*)^2$. The onset of substrate effects for the data given in Figs. 3–11 can be correlated by the relation

$$\tau_r^* > \frac{n^2}{50}(\tau_0^*/\omega^*)^2 \qquad (13)$$

Substrate effects depend on both the optical depth and optical radius as well as the albedo and the refractive index. They are important for all combinations of τ_0^*, τ_r^*, ω^*, and n that lie above the line shown in Fig. 12. The larger τ_r^* is relative to the right-hand side of Eq. (13), the greater the effects of the substrate on the backscattered radiation.

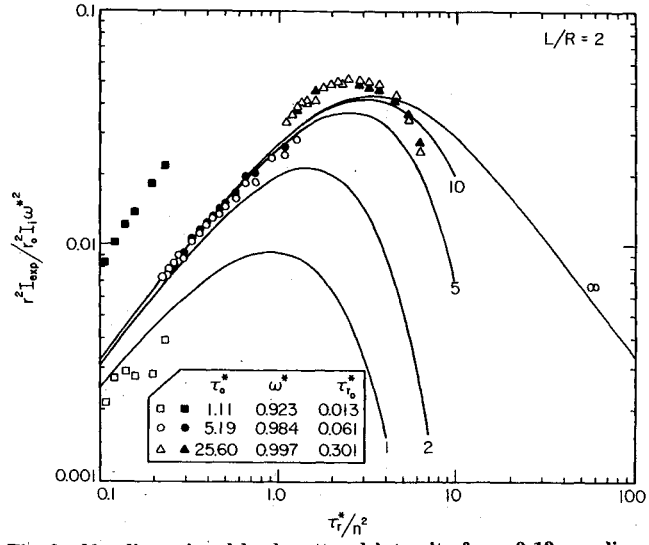

Fig. 9 Nondimensional backscattered intensity from 0.18 μm diam polystyrene latex particles in distilled water vs the contracted effective optical radius. ($L = 17$ cm; $R = 8.5$ cm; solid symbols, white substrate; open symbols, black substrate).

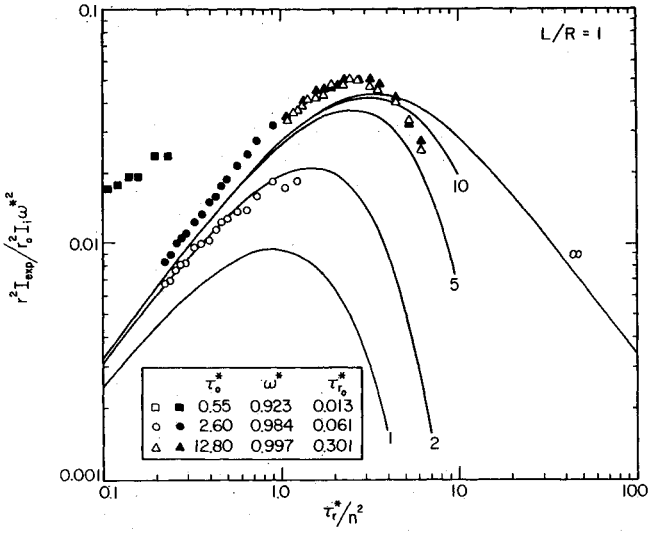

Fig. 10 Nondimensional backscattered intensity from 0.18 μm diam polystyrene latex particles in distilled water vs the contracted effective optical radius. ($L = 8.5$ cm; $R = 8.5$ cm; solid symbols, white substrate; open symbols, black substrate).

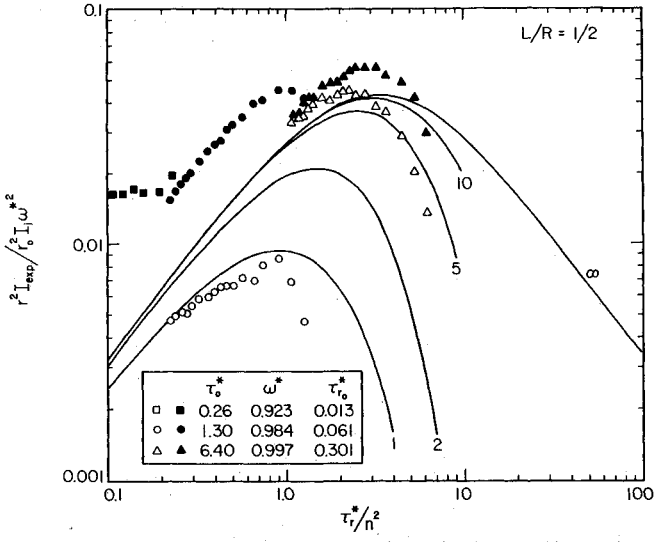

Fig. 11 Nondimensional backscattered intensity from 0.18 μm diam polystyrene latex particles in distilled water vs the contracted effective optical radius. ($L = 4.25$ cm; $R = 8.5$ cm; solid symbols, white substrate; open symbols, black substrate).

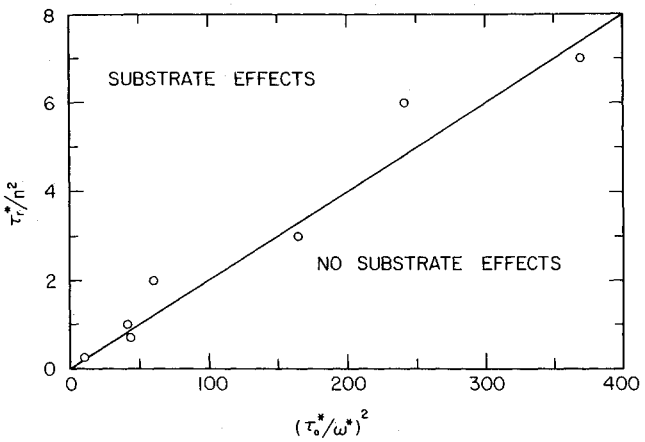

Fig. 12 Substrate effect boundary. Substrate effects are important for points above the curve.

Comparison of Experiment and Theory

Figures 3–11 show a comparison of experimental results for both the black and white substrates. In addition, the theory for a black substrate is shown for reference. In general, backscattered radiation from the medium with the black substrate agrees with the theory much better than that from the medium with the white substrate. This is to be expected, because the theory is for a nonparticipating substrate. All the experimental data of Figs. 3 and 7 show reasonable agreement with the theory. The data are slightly high relative to theory near τ_r^*/n^2 equal to 2 and fall off much faster than theory at values of τ_r^*/n^2 greater than 5. This is consistent with our previous results.[10] At small values of τ_0^*, as shown in Figs. 4–6 and 8–11, the black substrate experimental results generally follow the trends of the theory, except for the slightly higher and slightly displaced peak near τ_r^*/n^2 equal to 2 and the rapid fall-off with τ_r^* at τ_r^*/n^2 greater than 5. The white substrate results are always higher than the black substrate results for the same scattering medium when the substrate effects are noticeable.

Conclusions

1) The black substrate data agree reasonably well with the theory as they should, since the theory only holds for this substrate. This substantiates the experimental method and magnitude of the experimental parameters.

2) The effects of changing the substrate from black to white are most apparent for small τ_0^* near the laser beam (τ_r^* small); however, they still appear at large τ_r^* ($\simeq$ 10–15) for τ_0^* values of 20 and greater. All of this occurs at small L/R.

3) Substrate effects are evident if τ_r^* is greater than $(n\tau_0^*/\omega^*)^2/50$; if τ_r^* is smaller than this, the characteristics of the substrate are obscured.

Acknowledgment

This work has been supported in part by the National Science Foundation Grant CBT 85-01099. The authors thank Dr. A. L. Crosbie for many helpful suggestions and discussions.

References

[1]Crosbie, A.L. and Dougherty, R.L., "Two-Dimensional Isotropic Scattering in a Semi-Infinite Cylindrical Medium," *Journal of Quantitative Spectrosocopy and Radiative Transfer,* Vol. 20, Aug. 1978, pp. 151–173.

[2]Crosbie, A.L. and Dougherty, R.L., "Two-Dimensional Linear Anisotropic Scattering in a Semi-Infinite Cylindrical Medium Exposed to a Laser Beam," *Journal of Quantitative Spectroscopy and Radiative Transfer,* Vol. 28, Aug. 1982, pp. 233–264.

[3]Crosbie, A.L. and Dougherty, R.L., "Two-Dimensional Rayleigh Scattering in a Semi-Infinite Cylindrical Medium Exposed to a Laser Beam," *Journal of Quantitative Spectroscopy and Radiative Transfer,* Vol. 30, Sept. 1983, pp. 255–280.

[4]Crosbie, A.L. and Dougherty, R.L., "Two-Dimensional Isotropic Scattering in a Finite Thick Cylindrical Medium Exposed to a Laser Beam," *Journal of Quantitative Spectroscopy and Radiative Transfer,* Vol. 27, Feb. 1982, pp. 149–183.

[5]Crosbie, A.L. and Dougherty, R.L., "Two-Dimensional Linearly Anisotropic Scattering in a Finite Cylindrical Medium Exposed to a Laser Beam," *Journal of Quantitative Spectroscopy and Radiative Transfer,* Vol. 33, May 1985, pp. 487–520.

[6]Look, D.C., Nelson, H.F., and Crosbie, A.L., "Anisotropic Two-Dimensional Scattering, Comparison of Experiment with Theory," *ASME Journal of Heat Transfer,* Vol. 103, Feb. 1981, pp. 127–134.

[7]Look, D.C. and Sundvold, P.D., "Anisotropic Two-Dimensional Scattering Part II: Finite Depth and Refractive Index Effects," *AIAA Journal,* Vol. 22, April 1984, pp. 571–572.

[8]Look, D.C. and Sundvold, P.D., "Anisotropic 2-D Scattering 3: The Effects of Incident Laser Wavelength," *Applied Optics,* Vol. 23, Jan. 1984, pp. 9–11.

[9]Ishimaru, A., Kuga, Y., Cheung, R.L.T., and Shimizu, K., "Scattering and Diffusion of a Beam Wave in Randomly Distributed Scatters," *Journal of the Optical Society of America,* Vol. 73, Feb. 1983, pp. 131–136.

[10]Nelson, H.F., Look, D.C., Jr., and Crosbie, A.L., "Two-Dimensional Radiative Back-Scattering From Optically Thick Media," *ASME Journal of Heat Transfer,* Vol. 108, Aug. 1986, pp. 619–625.

[11]Ready, J.T., *Effects of High-Power Laser Radiation,* Academic Press, NY, 1971.

[12]Nelson, H.F., "Angular Distribution of Radiative Scattering: Comparison of Experiment and Theory," *AIAA Journal,* Vol. 19, March 1981, pp. 412–414.

[13]Van de Hulst, H.C., *Multiple Light Scattering,* Vol. 2, Academic Press, New York, 1980, Chaps. 10 and 14.

[14]Joseph, J.H. and Wiscombe, W.J., "The Delta-Eddington Approximation for Radiative Flux Transfer," *Journal of the Atmospheric Sciences,* Vol. 33, Sept. 1976, pp. 2452–2459.

[15]Hansen, J.E., "Exact and Approximate Solutions for Multiple Scattering by Cloudy and Hazy Planetary Atmospheres," *Journal of Atmospheric Sciences,* Vol. 26, May 1969, pp. 478–487.

[16]Potter, J.F., "The Delta Function Approximation in Radiative Transfer Theory," *Journal of Atmospheric Sciences,* Vol. 27, Sept. 1970, pp. 943–949.

[17]Wang, L., "Anisotropic Nonconservative Scattering in a Semi-Infinite Medium," *The Astrophysical Journal,* Vol. 174, June 1972, pp. 671–678.

[18]Sobolev, V.V., *Light Scattering in Planetary Atmosphere,* Pergamon, New York, 1975, pp. 158–161.

[19]Zuev, V.E., *Propagation of Visible and Infrared Radiation in the Atmosphere,* Wiley, New York, 1974, Appendix 2, p. 371.